molecular pharmaceutics

Article

Cite This: Mol. Pharmaceutics 2018, 15, 5349−5360

pubs.acs.org/molecularpharmaceutics

Polymorphism in Simvastatin: Twinning, Disorder, and Enantiotropic Phase Transitions

Ricardo G. Simões,[†] Carlos E. S. Bernardes,[†] Abhinav Joseph,[†] M. Fátima M. Piedade,[†,‡] Werner Kraus,[§] Franziska Emmerling,[§] Hermíno P. Diogo,[‡] and Manuel E. Minas da Piedade*[,†]

[†]Centro de Química e Bioquímica e Centro de Química Estrutural, Faculdade de Ciências Universidade de Lisboa, Campo Grande, 1749-016 Lisboa, Portugal

[‡]Centro de Química Estrutural, Instituto Superior Técnico, Universidade de Lisboa, 1049-001 Lisboa, Portugal

[§]BAM Federal Institute for Materials Research and Testing, Richard-Willstaetter-Strasse 11, 12489 Berlin, Germany

Supporting Information

ABSTRACT: Simvastatin is one of the most widely used active pharmaceutical ingredients for the treatment of hyperlipidemias. Because the compound is employed as a solid in drug formulations, particular attention should be given to the characterization of different polymorphs, their stability domains, and the nature of the phase transitions that relate them. In this work, the phase transitions delimiting the stability domains of three previously reported simvastatin forms were investigated from structural, energetics, and dynamical points of view based on single crystal X-ray diffraction (SCXRD), hot stage microscopy (HSM), and differential scanning calorimetry (DSC) experiments (conventional scans and heat capacity measurements), complemented with molecular dynamics (MD) simulations. Previous assignments of the crystal forms were confirmed by SCXRD: forms I and II were found to be orthorhombic ($P2_12_12_1$, $Z'/Z = 1/4$) and form III was monoclinic ($P2_1$, $Z'/Z = 2/4$). The obtained results further indicated that (i) the transitions between different forms are observed at 235.9 ± 0.1 K (form III → form II) and at 275.2 ± 0.2 K (form II → form I) in DSC runs carried out at 10 K min^{-1} and close to these values when other types of techniques are used (e.g., HSM). (ii) They are enantiotropic (i.e., there is a transition temperature relating the two phases before fusion at which the stability order is reversed), fast, reversible, with very little hysteresis between heating and cooling modes, and occur under single crystal to single crystal conditions. (iii) A nucleation and growth mechanism seems to be followed since HSM experiments on single crystals evidenced the propagation of an interface, accompanied by a change of birefringence and crystal contraction or expansion (more subtle in the case of form III → form II), when the phase transitions are triggered. (iv) Consistent with the reversible and small hysteresis nature of the phase transitions, the SCXRD results indicated that the molecular packing is very similar in all forms and the main structural differences are associated with conformational changes of the "ester tail". (v) The MD simulations further suggested that the tail is essentially "frozen" in two conformations below the III → II transition temperature, becomes progressively less hindered throughout the stability domain of form II, and acquires a large conformational freedom above the II → I transition. Finally, the fact that these transitions were found to be fast and reversible suggests that polymorphism is unlikely to be a problem for pharmaceutical formulations employing crystalline simvastatin because, if present, the III and II forms will readily convert to form I at ambient temperature.

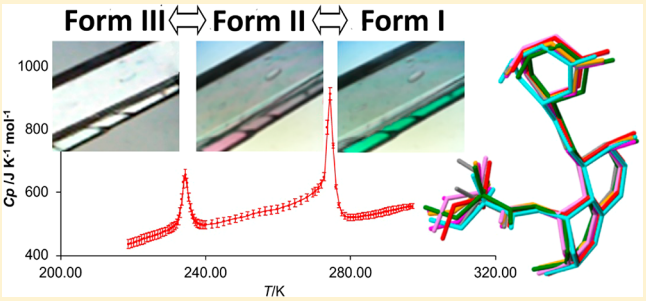

KEYWORDS: *simvastatin, polymorphism, twinning, disorder, phase transition, thermodynamics, DSC, hot stage microscopy, X-ray diffraction, MD simulations*

INTRODUCTION

Simvastatin (Figure 1, $C_{25}H_{38}O_5$, CAS No. 79902−63−9, 1*S*,3*R*,7*S*,8*S*,8a*R*)-8-{2-[(2*R*,4*R*)-4-hydroxy-6-oxotetrahydro-2*H*-pyran-2-yl]ethyl}-3,7-dimethyl-1,2,3,7,8,8a-hexahydronaphthalen-1-yl 2,2-dimethylbutanoate) is one of the most widely prescribed statins, a class of drugs especially designed to reduce the levels of low density lipoprotein cholesterol (LDL-c) particles, commonly dubbed "bad cholesterol".[1,2] Many studies have suggested that high LDL-c levels in humans are a major risk factor for the development of coronary heart diseases caused by arteriosclerosis,[3] a condition that is characterized by the clogging and hardening of arteries induced to a great extent by the buildup of LDL-c deposits in their inner walls. By lowering LDL-c levels, therapies based on simvastatin and other statins have significantly contributed to the prevention and treatment of such diseases.[4−6]

Received: August 1, 2018
Revised: September 5, 2018
Accepted: September 19, 2018
Published: September 19, 2018

DOI: 10.1021/acs.molpharmaceut.8b00818
Mol. Pharmaceutics 2018, 15, 5349−5360

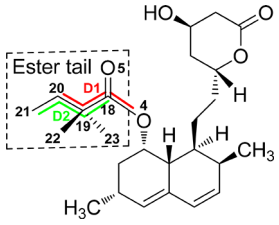

Figure 1. Molecular structure of simvastatin and labeling scheme of the heavy atoms and dihedral angles in the ester tail.

Simvastatin is normally incorporated as a solid in drug formulations and it is well-known that, in this case, particular attention should be paid to the tendency of the active pharmaceutical ingredient (API) to exist in different polymorphic forms (i.e., solid phases differing in the arrangement of the molecules in the crystal structure).[7−10] Indeed, because modifications of crystal packing may be accompanied by significant changes in physical properties, the lack of control over polymorphism may lead to serious problems in terms of reproducible preparation and safe use of an API.[7−10]

A previous study from our laboratories, which combined results of combustion calorimetry and heat capacity measurements by differential scanning calorimetry (DSC) with molecular dynamics (MD) simulations and quantum chemistry calculations, showed no evidence of polymorphism in simvastatin from ambient temperature (293 K) to the fusion temperature (DSC onset temperature, T_{on} = 412.2 ± 0.2 K).[11] The experiments indicated that the orthorhombic phase stable at ambient temperature (form I)[12,13] did not undergo any solid−solid phase transition within this temperature range, and the MD results suggested that only a progressive loss of conformational preference of the molecule ester tail (Figure 1) occurred as the temperature increased.

Two phase transitions have, however, been detected for simvastatin at subambient temperatures in a study combining DSC, X-ray diffraction, and solid state NMR experiments:[13,14] form III → form II at ∼232 K and form II → form I at ∼272 K. The diffraction experiments (single crystal X-ray diffraction, SCXRD, for form I[13] and X-ray powder diffraction using synchrotron radiation, XRPD-SR, for forms II and III[14]) indicated that the crystal structures of the three forms were similar. However, while forms I and II were both orthorhombic, space group $P2_12_12_1$, and had only one molecule in the asymmetric unit (Z'/Z = 1/4), form III was monoclinic, space group $P2_1$, and had two molecules in the asymmetric unit (Z'/Z = 2/4). ^{13}C solid-state cross-polarization/magic-angle-spinning nuclear magnetic resonance spectroscopy (^{13}C CP/MAS NMR) further suggested that the transitions between the three phases were essentially due to changes in the molecular conformations of the simvastatin ester tail,[14] a conclusion that is also consistent with a more recent terahertz time-domain spectroscopy (THz-TDS) investigation.[15]

Here, the structural and energetic changes associated with the low temperature phase transitions of simvastatin were investigated through a combined SCXRD, calorimetry, hot stage microscopy, and MD simulation approach. Insights into the molecular conformations and packing relationships between the different polymorphs and, in particular, on how differences in rotational freedom of the simvastatin ester tail in different temperature domains lead to pseudomerohedral twinning in the case of form III and disorder in the higher temperature forms are provided. The overall results also suggest that polymorphism is unlikely to originate problems in the manufacture of simvastatin formulations since both phase transitions are fast and reversible.

MATERIALS AND METHODS

Materials. The simvastatin sample (Jubilant Organosys) used in the differential scanning calorimetry experiments and in the preparation of crystals for hot stage microscopy and single crystal X-ray diffraction analysis had been characterized in terms of chemical purity, phase purity, and morphology by a variety of methods, namely, elemental analysis, HPLC-ESI/MS, diffuse reflectance infrared Fourier-transform (DRIFT) spectroscopy, ^{1}H and ^{13}C NMR, optical rotation, X-ray powder diffraction (XRPD), scanning electron microscopy (SEM), DSC, and thermogravimetry.[11] The XRPD results showed that the material corresponded to form I simvastatin and the HPLC-ESI/MS analysis led to a purity of 98.88 ± 0.12% in terms of molar percentage. Specific optical rotation measurements indicated that the sample consisted of ∼98% (+) isomer.

Crystals suitable for hot stage microscopy and single crystal X-ray diffraction studies (Figure 2) were obtained by adding

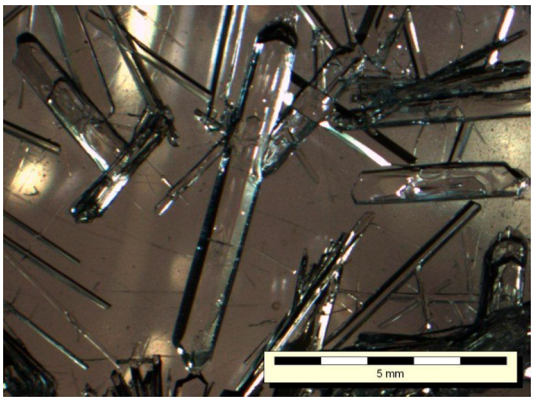

Figure 2. Optical microscopy image at 292 K of the simvastatin crystals used in the single crystal X-ray diffraction studies. The image was obtained with an Olympus SZX10 stereoscopic microscope and the Cell^D 2.6 software.

10 cm^3 of *n*-hexane (Panreac, 99.0%) to a solution of 1.2447 g of simvastatin in 4 cm^3 of acetone (Lab-Scan, 99.5%) prepared at room temperature (292 ± 2 K). The solution was contained in a 50 cm^3 beaker covered with aluminum foil. Hexane was added from a Crison Multi-Burette 4S through a needle inserted in the aluminum foil, at a rate of 0.02 cm^3 min^{-1}. The solution was left to evaporate at ambient temperature for 5 days, without removing the aluminum cover, and the obtained crystals were separated from the solvent by decantation, washed with distilled water and dried in air.

Single Crystal X-ray Diffraction Analysis. Single crystal X-ray diffraction studies were carried on a D8 Venture diffractometer (Bruker AXS, Germany) equipped with an APEX CCD area detector. Data collection was done on cooling at 298 ± 2 K, 260 ± 2 K, 253 ± 2 K, 200 ± 2 K, and 172 ± 2 K, and on heating at 253 ± 2 K and 298 ± 2 K. The temperature scale of the apparatus was previously calibrated against a TC Mess- and Regeltechnik type T thermocouple (0.5 mm diameter) placed at the same position as the crystal and connected to an Omega RDXL6SD data logger. An IμS X-ray source with a multilayer optic monochromated for Mo $K\alpha$ (λ = 0.71073 Å) radiation, operating at 50 kV and 1 mA, was used. An empirical absorption correction was applied by using Bruker SADABS,[16] and the data

DOI: 10.1021/acs.molpharmaceut.8b00818
Mol. Pharmaceutics 2018, 15, 5349−5360

Table 1. Crystal Data and Structure Refinement Parameters for Simvastatin at Various Temperatures

T/K	172 ± 2	200 ± 2	253 ± 2	260 ± 2	298 ± 2
polymorph	form III	form III	form II	form II	form I
cryst syst	monoclinic	monoclinic	orthorhombic	orthorhombic	orthorhombic
space group	$P2_1$	$P2_1$	$P2_12_12_1$	$P2_12_12_1$	$P2_12_12_1$
a/Å	5.9874(5)	6.0018(6)	6.0524(2)	6.0587(3)	6.1145(2)
b/Å	16.1056(15)	16.139(2)	16.3826(5)	16.4386(10)	17.2901(6)
c/Å	23.4443(19)	23.448(3)	23.4238(7)	23.3475(14)	22.4334(8)
β/deg	90.04(2)	90.032(7)			
V/Å^3	2260.7(3)	2271.2(5)	2322.56(13)	2325.3(2)	2371.67(14)
Z, Z'	4, 2	4, 2	4, 1	4, 1	4, 1
ρ_{calcd}/g cm^{-3}	1.230	1.224	1.197	1.196	1.172
μ/mm^{-1}	0.084	0.083	0.082	0.081	0.080
F(000)	912	912	912	912	912
θ limits/deg	2.529−28.321	2.524−28.383	2.486−28.325	2.478−28.301	2.356−28.317
limiting indices	$-7 \le h \le 7$	$-8 \le h \le 8$	$-8 \le h \le 7$	$-8 \le h \le 7$	$-7 \le h \le 8$
	$-21 \le k \le 21$	$-21 \le k \le 21$	$-21 \le k \le 21$	$-21 \le k \le 21$	$-23 \le k \le 23$
	$-31 \le l \le 31$	$-31 \le l \le 31$	$-31 \le l \le 31$	$-314 \le l \le 31$	$-29 \le l \le 29$
reflns collected/unique	56343/11092 [R(int) = 0.0689]	52913/11185 [R(int) = 0.1162]	51602/5742 [R(int) = 0.0914]	68995/5759 [R(int) = 0.2277]	53096/5878 [R(int) = 0.1042]
completeness to θ/%	99.8	99.8	99.5	99.7	99.6
data/restraints/parameters	11092/1/541	11185/1/541	5742/2/290	5759/0/339	5878/0/271
GOF on F^2	1.032	1.087	1.101	1.064	1.083
final R indices [$I > 2\sigma(I)$]	R_1 = 0.0476	R_1 = 0.0590	R_1 = 0.0672	R_1 = 0.1079	R_1 = 0.0789
R indices (all data)	R_1 = 0.0638	R_1 = 0.0812	R_1 = 0.0944	R_1 = 0.2085	R_1 = 0.1172
largest diff. peak and hole/e Å^{-3}	0.219 and −0.293	0.251 and −0.290	0.216 and −0.247	0.381 and −0.399	0.307 and −0.280

reduction was performed with Bruker SAINT.[17] Structures were solved by direct methods with Bruker SHELXTL[18] and refined by full-matrix least-squares on F^2 using the SHELXL97[19] program included in WINGX-Version 1.80.05.[20] Non-hydrogen atoms were refined with anisotropic thermal parameters. The hydrogen atoms were inserted in calculated positions and allowed to refine riding on the parent carbon atom with a $U_{iso}(H) = 1.2U_{eq}(C)$. The twin nature of form III (the phase stable at 172 and 200 K) became apparent after attempting to solve the structure in an orthorhombic unit cell because the data were of good quality but an inexplicable high R factor persisted. The twinning was not immediately recognized because (i) the twin structure is pseudomerohedral with $\beta \approx 90°$ and a twinning fraction $x = 0.5$; (ii) other common signs of twinning, such as $|E^2 - 1|$, had normal values between 0.736 and 0.968 for acentric and centric structures, respectively; and (iii) from the diffraction patterns no splitting of the spots was detected. The twin law [1 0 0; 0−1 0; 0 0−1] applied to the two equal domains ($x = 0.5$) to correct the intensities of the overlapping reflections was found using PLATON (TwinRotMat). Structural representations were prepared using Mercury 3.10.1.[21] PLATON was used for the hydrogen bond interactions.[22] A summary of the crystal data, structure solution, and refinement parameters is given in Table 1. Only data referring to the cooling mode are shown since no significant differences were noted for those collected on heating. The obtained absolute structure parameters were meaningless because the compound is a weak anomalous scatterer. They were, therefore, removed from the CIF files and it was assumed that the enantiomer that was determined was that corresponding to optical rotation measurements (see above).

Differential Scanning Calorimetry (DSC). Conventional DSC scans were carried out on a TA Instruments 2920 MTDSC apparatus. The samples, with masses in the range 2−3 mg, were sealed under air, in aluminum pans, and weighed to ±0.1 μg on a Mettler UMT2 ultramicro balance. Helium (Air Liquide N55) at a flow rate of 0.5 cm^3 s^{-1} was used as the purging gas. The heating rate (β) was 4 K min^{-1} or 10 K min^{-1}. The temperature calibration was performed at those same heating rates by taking the onset of the fusion peaks of the following standards: n-decane (Fluka, > 99.8%; T_{fus} = 243.75 K), n-octadecane (Fluka, > 99.9%; T_{fus} = 301.77 K), hexatriacontane (Fluka, > 99.5%; T_{fus} = 347.30 K), indium (TA Instruments, DSC standard; T_{fus} = 430.61 K), and tin (TA Instruments, DSC standard; T_{fus} = 506.03 K). The heat flow scale of the instrument was calibrated with indium ($\Delta_{fus}h$ = 28.71 J g^{-1}).

Heat capacity measurements in the range 218 to 297 K were performed on a Netzsch 204 F1 Phoenix apparatus equipped with an intracooler system. The instrument control and all data treatment procedures were performed with the Netzsch Proteus Software V. 6.1.0. The samples with masses of ∼13 mg, were contained in aluminum crucibles and were weighed with a precision of ±0.1 μg on a Mettler XP2U ultramicrobalance. Nitrogen (Linde N_2 5.0) was used both as purge (flow rate: 20 cm^3 min^{-1}) and protective gas (flow rate: 70 cm^3 min^{-1}). All experiments were carried out at a heating rate β = 10 K min^{-1}. The temperature and energy scales of the apparatus were calibrated at the same heating rate, using a calibration kit from Netzsch (ref 6.239.2−91.3.00), consisting of adamantane (99%, T_{trs} = 208.65 K, $\Delta_{trs}h$ = 22.0 J g^{-1}), indium (99.999%, T_{fus} = 429.75 K, $\Delta_{fus}h$ = 28.6 J g^{-1}), tin (99.999%, T_{fus} = 505.05 K, $\Delta_{fus}h$ = 17.2 J g^{-1}), bismuth (99.999, T_{fus} = 544.55 K, $\Delta_{fus}h$ = 53.1 J g^{-1}), zinc (99.999, T_{fus} = 692.65 K, $\Delta_{fus}h$ = 107.5 J g^{-1}), and cesium chloride (99.999, T_{fus} = 749.15 K, $\Delta_{fus}h$ = 17.2 J g^{-1}). The heat capacity measurements were performed in the continuous mode,[23] using sapphire (Netzsch ref 6.239.2−91.5.00, Al_2O_3 disks, 99.99%) as reference. The experimental procedure has been described,[24] and involved a sequence of three runs carried out with the same temperature program and the same pair of crucibles: a blank run with empty reference and sample crucibles; a second run carried out with sapphire in the sample

DOI: 10.1021/acs.molpharmaceut.8b00818
Mol. Pharmaceutics 2018, 15, 5349−5360

crucible; and a third run with simvastatin in the sample crucible. The standard molar heat capacities of simvastatin, $C^{o}_{p,m}$, were computed by using the C_p ratio method,[24] implemented in the Netzsch Proteus Analysis software Version 6.1.0. An accuracy test carried out with benzoic acid in the temperature range 219 to 272 K, with β = 10 K min^{-1}, showed that the method used in this work led to a maximum deviation of 3.1% between the obtained $C^{o}_{p,m}$ results and benchmark adiabatic calorimetry data[25] (see Supporting Information, Table S3).

Hot Stage Microscopy (HSM). Hot stage microscopy studies of the solid−solid phase transitions between the different simvastatin polymorphs were performed on an Olympus Bx51 optical transmission microscope. The apparatus was equipped with an Olympus C5060 wide zoom camera and a Linkam LTS360 liquid nitrogen-cooled cryostage, which allows experiments in the 123−573 K temperature range, either in isothermal or ramp modes. A simvastatin crystal was placed between two microscope slides, inserted in the hot stage, and observed under nonpolarized light. Images were recorded on cooling and heating in the same temperature regions where the phase transitions were detected by DSC. The heating/cooling rates and magnifications were 5 K min^{-1} and 100× for the I ↔ II phase transition, and 10 K min^{-1} and 500× for the II ↔ III phase transition.

Molecular Dynamic (MD) Simulations. The MD simulations were carried out with GROMACS 2016.4.[26] A cutoff distance of 15 Å was selected for all calculations. The Particle-Mesh Ewald electrostatics technique with a Fourier grid spacing of 0.06 nm was applied to account for interactions beyond that distance. The simulations were performed at a pressure of 1 bar, by using an anisotropic Parrinello−Rahman barostat, with the six compressibility components set to 1 × 10^{-6} bar^{-1} and a time constant of 10 ps. The temperature was controlled with a V-rescale thermostat using a time constant of 1 ps. The following heating protocol was used: (i) the initial simulation box (see details below) was equilibrated at 140 K for 1 ns; (ii) after equilibration, a production run of 20 ns was performed, where the configuration of the system was recorded each 200 ps for subsequent analysis; (iii) the temperature of the system was increased by 10 K and the previous two steps were repeated until a temperature of 300 K was reached.

Crystalline simvastatin was modeled in a simulation box containing 168 molecules (11 424 atoms), initially packed according to the twin structure of form III determined in this work at 172 K (Table 1), where two molecules with conformations *A* and *B* are present in the unit cell. Several unit cells were stacked along the three axes (7 × 3 × 2) to create a well-proportioned supercell, capable of accommodating the 15 Å cutoff. The force field previously used for solid and liquid simvastatin in the range 293−413 K[11] was adopted. The functional form and parametrization of the van der Waals interactions and of the intramolecular motions related to changes in bond distances, bond angles, and dihedral angles were directly borrowed from the OPLS-AA model.[27,28] The Coulombic interactions were based on atomic point charges calculated as described elsewhere.[11] All input files necessary to run GROMACS were prepared with DLPGEN 2.1.0.[29] The analysis of the distributions of D1 and D2 dihedral angles for all molecules in the simulation box, and for a total of 10 000 recorded frames was performed using AGGREGATES.[30]

RESULTS AND DISCUSSION

All molar quantities were based on the previously used molar mass of simvastatin M = 418.5662 g mol^{-1},[11] which relies on the standard atomic masses recommended by the IUPAC Commission in 2013.[31]

DSC Studies. Two well-defined solid−solid phase transitions were observed for simvastatin by DSC in the range 193 to 320 K, thus corroborating previous findings.[14] This is illustrated in Figure 3 for an experiment consisting of two sequential cooling and heating runs performed with the same sample, at scan rates of (a) 4 K min^{-1} and (b) 10 K min^{-1} (detailed results are given as Supporting Information).

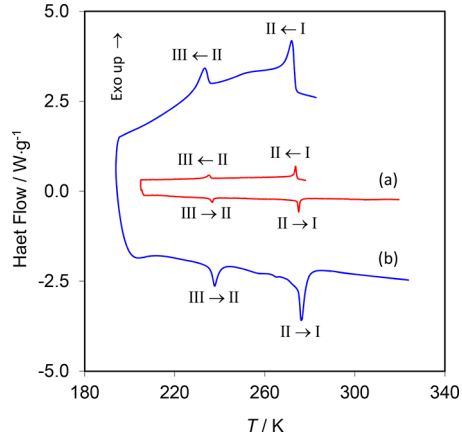

Figure 3. Differential scanning calorimetry measured curves for a crystalline simvastatin sample of mass m = 2.367 mg in two consecutive cooling/heating cycles at rates of (a) 4 K min^{-1} (red line) and (b) 10 K min^{-1} (blue line).

The onset (T_{on}) and maximum (T_{max}) temperatures of the solid−solid phase transition peaks and the corresponding molar enthalpies ($\Delta_{trs}H_m$) and entropies ($\Delta_{trs}S_m = \Delta_{trs}H_m/T_{on}$), obtained at a heating rate of 10 K min^{-1} were: (i) for the III → II transition, T_{on} = 235.9 ± 0.1 K, T_{max} = 237.4 ± 0.2 K, $\Delta_{trs}H_m$ = 0.95 ± 0.06 kJ mol^{-1}, and $\Delta_{trs}S_m$ = 4.0 ± 0.2 J K^{-1} mol^{-1}; (ii) for the II → I transition, T_{on} = 275.2 ± 0.2 K, T_{max} = 276.0 ± 0.1 K, $\Delta_{trs}H_m$ = 3.3 ± 0.1 kJ mol^{-1}, and $\Delta_{trs}S_m$ = 12.0 ± 0.3 J K^{-1} mol^{-1}. The uncertainties assigned to T_{on}, T_{max}, $\Delta_{trs}H_m$, and $\Delta_{trs}S_m$ correspond to twice the standard errors of the mean of five determinations. The onset temperatures of the III → II and II → I phase transitions given above are slightly higher (~3 K) than those reported by Hušák et al.[14] (232 and 272 K for the III → II and II → I phase transitions, respectively) at the same heating rate. Note that in this publication the phase transitions are indicated to be endothermic on cooling and exothermic on heating, but this was later confirmed to be a typo and the actual results are in good agreement with those found in the present work.[32] Lower values than those here determined were also published, which corresponded to a single DSC scan carried out at 10 K min^{-1} (T_{on} = 230.9 K for the III → II and T_{on} = 270.7 K for II → I transitions)[15] or an analysis of THz-TDS data (231.4 and 274.6 K for the III → II and II → I phase transitions, respectively).[15]

Figure 3 also shows that the transitions were reversible and occurred with only small undercooling (0.2−1.2 K) in the cooling mode, regardless of the scan rate. In addition, at all rates, the phase transition enthalpies obtained on cooling and on heating differed by less than 0.1 kJ mol^{-1}.

The III → II and II → I phase transitions were further investigated through low temperature heat capacity measurements carried out by DSC (β = 10 K min^{-1}) in the temperature range 218−297 K. The results are compared in Figure 4 with

DOI: 10.1021/acs.molpharmaceut.8b00818
Mol. Pharmaceutics 2018, 15, 5349−5360

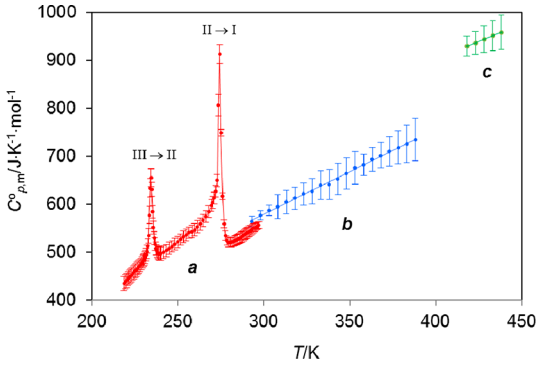

Figure 4. Low temperature heat capacity of solid simvastatin obtained in this work in the range 218−297 K (curve *a*, red) and heat capacities reported by Simões et al.[11] for solid (293−388 K, curve *b*, blue) and liquid (418−438 K, curve *c*, green).

previously reported data for the same sample, above ambient temperature, in the solid (293−388 K) and liquid (418−438 K) states.[11] Each data point in Figure 4 obtained in this work (curve *a*) is the mean of six independent determinations (see Supporting Information for details). For all plotted data (this work and literature), the indicated error bars represent twice standard errors of the mean of the number of independent determinations performed. The difference between the $C^{\circ}_{p,m}$ values of simvastatin obtained from curves *a* and *b* within their contact zone is ~3%, and is covered by the corresponding uncertainty intervals. This suggests a good internal consistency between the present (subambient temperature range) and previous (supra-ambient temperature range[11]) determinations, which were carried out on different instruments.

The peaks detected for the two solid−solid phase transitions in the DSC scans (Figure 3) were also observed in the heat capacity experiments (Figure 4), with maxima at an approximately 3 K lower temperature, namely, 234.4 K (III → II) and 274.4 K (II → I). The λ form of the heat capacity profile of both transitions, suggests that they are of order−disorder nature, with the disorder level slowly increasing within a specific phase domain until a somewhat abrupt change occurs when the nucleation of a new phase starts. This is particularly well illustrated by the long tail of the II → I peak, which extends over a large temperature range down to the end of the III → II transition. Furthermore, the fact that the undercoolings detected in the cooling/heating cycles shown in Figure 3 were small, and the III ↔ II and II ↔ I transitions were fast and reversible, points to low associated kinetic barriers. Such conclusions are in agreement with previous results from ^{13}C CP/MAS NMR[14] and THz-TDS[15] studies and are also consistent with the hot stage microscopy, SCXRD, and MD results discussed in the following sections.

Hot Stage Microscopy (HSM). As shown in Figure 5 and Videos 1−4 given in the Supporting Information, the occurrence of the phase transitions at approximately 235 K (form III → form II) and 275 K (form II → form I), under single crystal to single crystal conditions, was clearly evidenced by changes in the interference colors transmitted by the initial and final phases. These temperatures agree very well with those given by the DSC experiments (235.9 ± 0.1 K and 275.2 ± 0.2 K, respectively). Also in agreement with the DSC observations, the transitions were found to be reversible, since the initial color pattern could be completely restored by switching between heating and cooling modes. The change in interference color revealed the propagation of an interface throughout the phase transition, thus

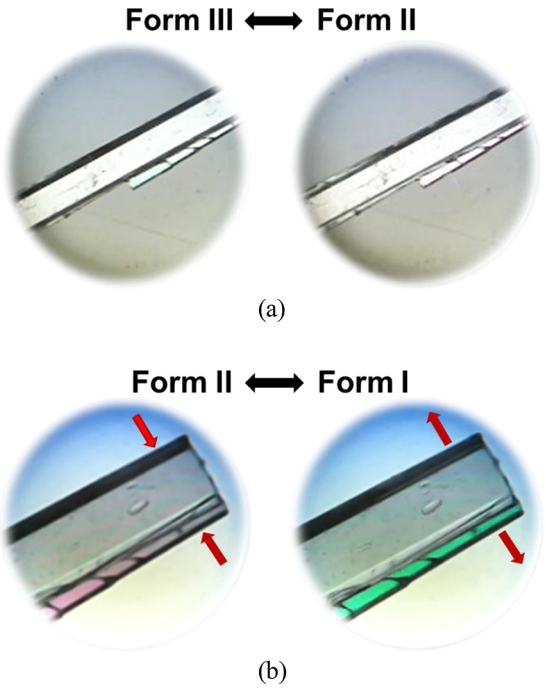

Figure 5. Hot stage microscopy images of (a) the III ↔ II and (b) II ↔ I phase transitions in simvastatin. The red arrows indicate the direction of crystal contraction or expansion associated with the II ↔ I process. The images of the two phase transitions were recorded with the same crystal but focusing on different regions.

suggesting a nucleation and growth mechanism. The sudden contraction of the smaller edge that accompanies the I → II transition (Figure 5) is compatible with the decrease of the unit cell *b* axis indicated by the SCXRD results in Table 1. The nonobservance of a similar effect for the II → III transition is not unexpected given the comparatively much smaller change in unit cell dimensions associated with the latter process. The fact that no fragmentation of the crystals was noted when they were subjected to repeated cooling/heating cycles within the regions where the phase transitions occur, suggests that they do not involve large structural changes, which might lead to the build up or release of considerable mechanical strain.

Structure. Single crystal X-ray diffraction analysis was carried out on cooling, at 298 ± 2 K, 260 ± 2 K, 253 ± 2 K, 200 ± 2 K, and 172 ± 2 K and on heating at 253 ± 2 K and 298 ± 2 K. As previously mentioned, no significant differences between the results obtained on cooling or heating modes were observed. Mercury 3.10.1[21] drawings of the simvastatin molecule at different temperatures, relevant for the discussion below are illustrated in Figure 6. The atom labeling scheme is given in Figure 6a and b.

As can be seen in Figure 6c the molecular conformations of the simvastatin molecule at different temperatures are very similar, except in what concerns the ester tail. The changes in mobility of the tail with temperature are reflected by variations in the torsion angles O4−C18−C19-C20 and C18−C19−C20-C21 (D1 and D2, respectively, in Figure 1). The obtained values of those angles for different temperatures are listed in Table 2. Also included in Table 2, for comparison purposes, are the analogous data previously reported from SCXRD at 293 K,[13] and by PXRD-SR at 150 and 258 K.[14] The observed differences probably reflect the "freezing" of the highly mobile ester tail at slightly different angles (note that the published conformations and those found here are highly superimposable for other parts

DOI: 10.1021/acs.molpharmaceut.8b00818
Mol. Pharmaceutics 2018, 15, 5349−5360

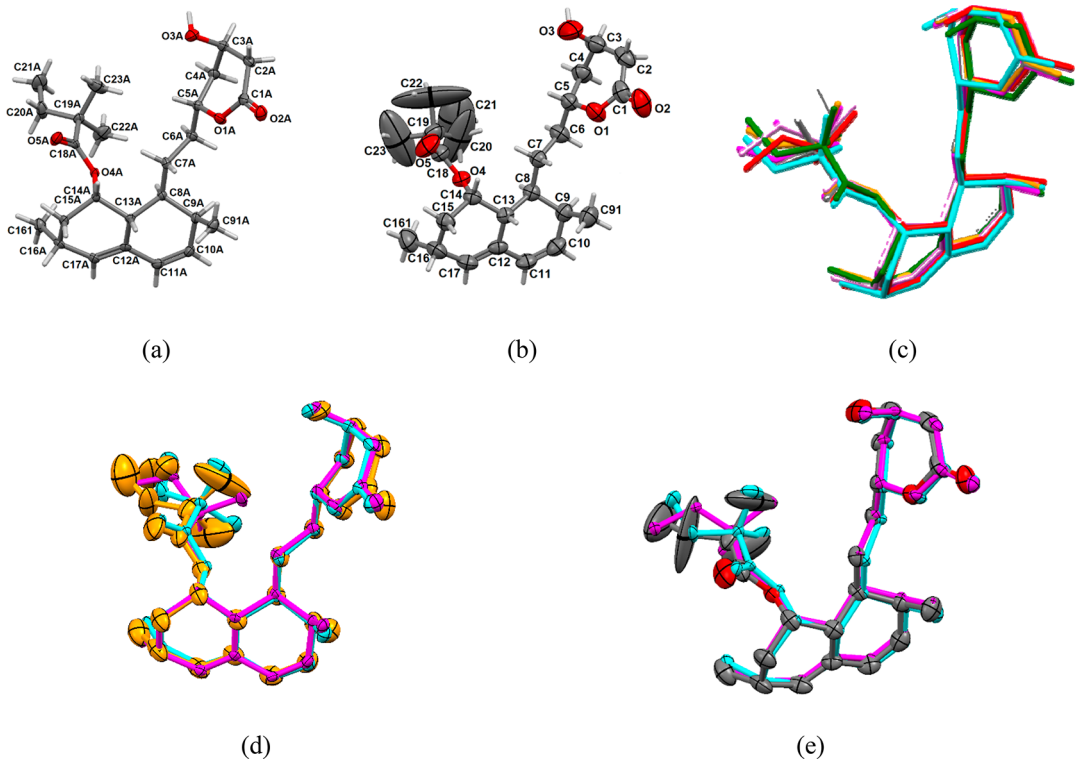

Figure 6. Mercury 3.10.1[21] drawings and labeling scheme of the simvastatin molecule for structures at (a) 172 K (twinned structure, molecule *A*) and (b) 260 K (nontwinned structure). (c) Overlay of the molecules in all simvastatin structures (hydrogen atoms removed) determined in this work, showing the different conformations of the ester tail as a function of temperature: 172 ± 2 K (cyan and red), 200 ± 2 K (violet and green), 253 ± 2 K (orange), 260 ± 2 K (magenta), and 298 ± 2 K (gray). (d) Overlay of the two molecules in the twinned form III structure at 172 K (cyan and magenta) and that in form II with resolved disorder at 253 K (orange); (e) analogous overlay for the form II molecule with unresolved disorder, at 260 K (gray).

Table 2. Torsion Angles of Ester Tail of Simvastatin (D1 and D2 in Figure 1) at Different Temperatures[a]

T/K	172 ± 2 K	200 ± 2 K	253 ± 2 K	260 ± 2 K	298 ± 2 K
form	III	III	II	II	I
O4−C18−C19-C20	175.1(3) *A*	175.2(4) *A*	175.4(6) *loc* (49%)[b]	143(1)	−22(1)
(D1)	128.5(4) *B*	129.6(5) *B*	130.5(6) *hoc* (51%)[b]		−26.3 *hoc*[b,c]
	48.3 *A*[d]			137.5[d]	155.2 *loc*[b,c]
	13.6 *B*[d]				
C18−C19−C20-C21	176.4(5) *A*	176.1(7) *A*	−120(1) *loc*(49%)[b]	−165.0(3)	−176(2)
(D2)	−71.4(5) *B*	−71.4(7) *B*	133(2) *hoc* (51%)[b]	−172.9[d]	174.8 *hoc*[b,c]
	−76.6 *A*[d]				138.4 *loc*[b,c]
	−166.7 *B*[d]				

[a]*A* and *B* denote each of the two molecules in the asymmetric unit of the pseudomerohedral twin structure; *hoc* and *loc* represent the high occupancy conformation and low occupancy conformation, respectively, in the disordered structures. [b]Structure with the disorder of the ester tail resolved. [c]SCXRD data at 293 K from refs 13 and 14 with disorder resolved. [d]PXRD-SR data at 150 K from ref 14.

of the molecule). One further relevant aspect is the fact that albeit the structural features of simvastatin form III are better captured by a pseudomerohedral twin model, the two molecules in the unit cell bear a strong conformational similarity with those corresponding to (*i*) form II at 253 K, where disorder was resolved (Figure 6d), and (*ii*) form II at 260 K, where disorder remained unresolved (Figure 6e). Note that in the latter case the ADPs of the atoms in the ester tail of the disordered form II molecule envelop the D1 and D2 dihedral angles of the two molecules in the twinned form III structure.

The SCXRD results indicated that forms I (stable above 275.2 K) and II (stable in the range 235.9−275.2 K) are orthorhombic, space group $P2_12_12_1$, with only one molecule in the asymmetric unit ($Z'/Z = 1/4$). As mentioned above, form III (stable below 235.9 K) corresponds to a pseudomerohedral twinned monoclinic structure (space group $P2_1$ with $Z'/Z = 2/4$), with a twin fraction $x = 0.5$. Consistent with the DSC and HSM results, the form I → form II and the form II → form III transitions were both found to be reversible and to occur under single crystal to single crystal conditions, without crystal fragmentation. Thus, the twinning phenomenon observed on cooling below the II → III phase transition temperature entirely disappears on heating and is not accompanied by a thermosalient effect (i.e., a jumping motion, an explosive behavior, or a dramatic change in shape of a crystal, triggered by a temperature stimulus) similar to that noted, for example, in the case of 1,2,4,5-tetrabromobenzene twins.[33]

The phase assignments here obtained are in agreement with the previous SCXRD study of form I at 293 K[13] and with the structures of forms II and III obtained from X-ray powder

DOI: 10.1021/acs.molpharmaceut.8b00818
Mol. Pharmaceutics 2018, 15, 5349−5360

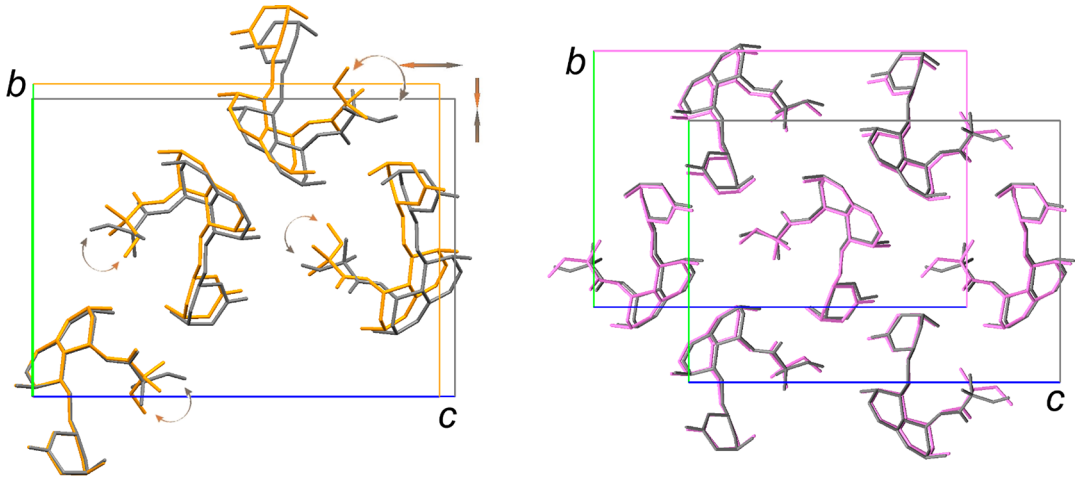

(a) (b)

Figure 7. (a) Overlay of the unit cells of simvastatin forms I (orange, 298 K) and II (gray, 260 K), showing the changes associated with the I → II phase transition. (b) Analogous overlay for the II → III phase transition (form II, gray, 260 K; form III, violet, 172 K).

diffraction experiments using synchrotron radiation, performed at 258 and 150 K, respectively.[14] In all forms, the thermal ellipsoids of the carbon atoms from the ester tail are very large compared to those of the atoms in the remaining molecular framework (see, for example, the form II molecule at 260 ± 2 K in Figure 6b). In the case of forms I and II, the application of a disorder model with refinement into two positions, as suggested by SHELX was, however, only successful for form II at 253 ± 2 K.

At the form I → form II transition a rotation of the most probable D1 dihedral angle of the ester tail by ∼160° is observed (Table 2 and Figure 7a) and the unit cell contracts in the direction of *b* from 17.29 to 16.38 Å (Table 1 and Figure 7a). As noted above, this may justify the contraction of the crystals in the direction of the smaller edge noted in the HSM experiments (Figure 5a and Videos 1 and 2 in the Supporting Information). An elongation of the *c*-axis from 22.43 to 23.42 Å also occurs.

The form II → form III transition is characterized by a change from an orthorhombic to a pseudomerohedral twinned monoclinic structure. The associated differences in unit cell dimensions are, however, much smaller when compared to the form II → form I transformation (Figure 7b), a feature which was also captured by the HSM experiments, where a crystal contraction/expansion is not evident (see Figure 5b and Videos 3 and 4 in the Supporting Information).

One of the signs of twinning in simvastatin form III (stable below 235.9 K) was the fact that the structures corresponding to higher temperatures could be solved as orthorhombic with good fitting but the orthorhombic fittings became poorer as the temperature decreased. When the structures of form III at 172 ± 2 K and 200 ± 2 K were analyzed with the intensities corrected for twinning, the thermal ellipsoids of the atoms in the ester tail became smaller and *R* factors at low temperature (Figures 6a) became better than those at higher temperatures (e.g., Figure 6b), where the structural disorder associated with the variety of the simvastatin ester tail conformations over a wide range of D1 and D2 dihedral angles is evident. Such disorder, which was also observed in previous work,[14] is reflected by the large atomic displacement parameters (ADP) of C20, C21, C22, and C23 (Figure 6b). To investigate the nature of this effect, several different models with these atoms disordered over two or more sites were tested, but most attempts resulted in unstable refinements. As mentioned above, only at 253 K the disorder model was successful. It can also be noted that, although the ADP's of those atoms are progressively reduced upon cooling from ambient temperature to 172 K, they are still very large compared to those of the remaining simvastatin atoms (see Figure 6a and CIF file given as Supporting Information). This may be originated by a dynamic disorder, which can, in principle, be minimized by cooling the crystal. Indeed, according to ^{13}C CP/MAS NMR evidence[14] and also from the MD simulations carried out in this work (see below), in form III the simvastatin ester tail is essentially frozen in two different conformations and the number of accessible conformations continuously increases as the temperature increases. Therefore, form III contains two symmetry independent molecules in the asymmetric unit and this leads to a loss of symmetry in the crystal structure. Consequently, the crystal structure is best described in the monoclinic space group $P2_1$ with a β angle very near 90° according to the group-subgroup transformation. To complete the missing part in the $P2_1$ structure solution, compared with the orthorhombic one, the structure exhibits a 2-fold axis as twin component [1 0 0; 0−1 0; 0 0−1], which is usually not present in this space group. The solution as a twin gives a very good *R*-value for the crystal structure of form III.

The major features of the simvastatin molecular packing were found to be similar at all temperatures probed by the SCXRD experiments, regardless of the twined or disordered nature of the polymorphs. As illustrated in Figure 8 for the 298 K structure, the molecules are arranged in infinite one-dimensional $C_1^1(13)$ chains along the *b* axis sustained by O3−H···O5 hydrogen bonds (Figure 8a). This corroborates previous findings at 293 K.[13] The structure extends as a two-dimensional (2D) sheet along *c* axis via C2−H···O2 contacts involving the carbonyl oxygen (O2) of the lactone ring as donor. The 3D packing, where the chains are arranged parallel to each other, is completed along the *a*-axis by the C9−H···O2 interaction (Figure 8b).

The variation of the hydrogen bond distances corresponding to the interactions mentioned above with temperature, is given in Table 3. The results show that between 170 and 298 K, the length of the O3−H···O5 hydrogen bond establishing the 1D infinite chains along the *b* axis steadily increases with temperature by ∼5%, a value which is identical to the corresponding

DOI: 10.1021/acs.molpharmaceut.8b00818
Mol. Pharmaceutics 2018, 15, 5349−5360

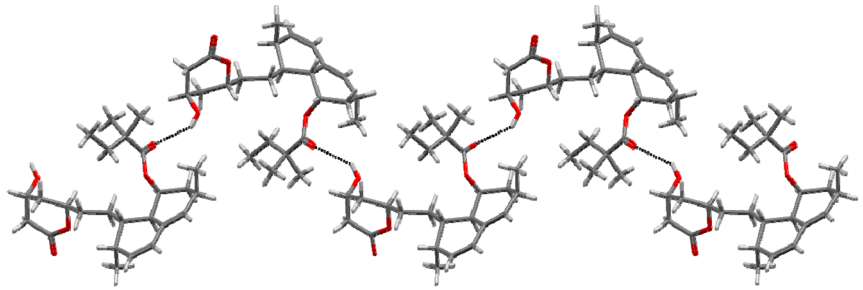

(a)

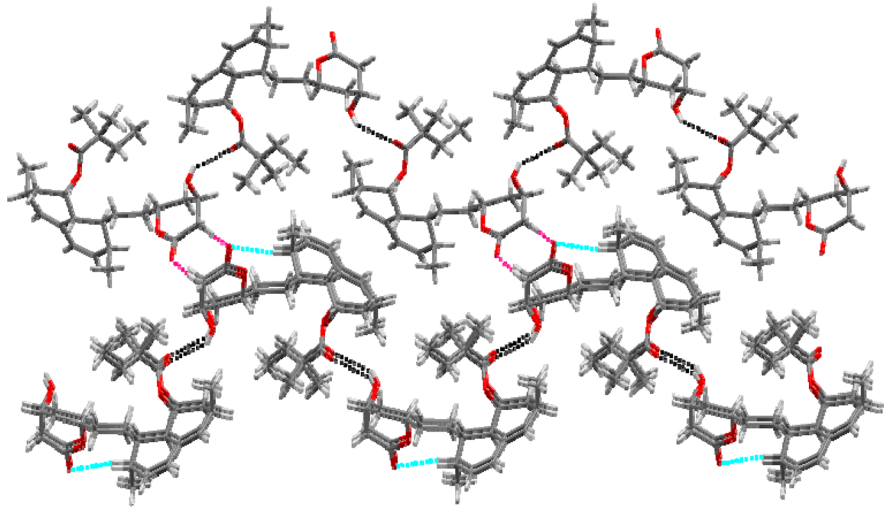

(b)

Figure 8. Molecular packing of simvastatin at 298 K: (a) infinite one-dimensional $C_1^1(13)$ chain along the *b* axis sustained by the O3−H···O5 hydrogen bond (black dashed lines); (b) complete 3D packing showing the C2−H···O2 interaction (pink dashed lines) and the C9−H···O2 (cyan dashed lines).

Table 3. Hydrogen Bond Distances (Å) in Crystalline Structures of Simvastatin at Different Temperatures

T/K	172 ± 2 K	200 ± 2 K	253 ± 2 K	260 ± 2 K	298 ± 2 K
O3−H···O5	2.12	2.01	2.13	2.13	2.16
	2.09	2.11			
C2−H···O2	2.49	2.49	2.51	2.51	2.49
	2.50	2.49			
C9−H···O2	2.57	2.43	2.51	2.46	2.52
	2.42	2.56			

unit cell volume expansion (Table 1). The distances of the weaker C2−H···O2 and C9−H···O2 interactions are similar to each other and approximately constant over the full temperature range covered by the experiments. It can therefore be concluded that, at the molecular level, the III ↔ II and II ↔ I transitions in simvastatin bear a stronger relationship with conformational changes of the ester tail (dihedral angles D1 and D2, Figure 1), than with changes in the hydrogen-bond network supporting the packing. This is compatible with the DSC results pointing to low associated kinetic barriers and with the reported findings of ^{13}C CP/MAS NMR[14] and THz-TDS.[15] It may also be pointed out that the number of van der Waals contacts involving the simvastatin ester tail atoms increases, and the corresponding interaction distances decrease along the sequence form I → form II → form III, thus suggesting that tail movements will be more difficult as the temperature becomes lower (see CIF file given as Supporting Information).

Molecular Dynamics Simulations. The MD simulations were able to capture the SCXRD unit cell parameters of simvastatin with average and maximum deviations of 1.2% and 4%, respectively (see Supporting Information). These deviations are similar to those found when the present force field was applied to simvastatin above ambient temperature.[11] They are also typical of the performance of other force-fields of similar type when validated against experimental crystal structure data.[27−29,34] The densities (ρ) obtained from the theoretically computed unit cell dimensions are compared in Figure 9 with the analogous experimental values in Table 1. The qualitative agreement

DOI: 10.1021/acs.molpharmaceut.8b00818
Mol. Pharmaceutics 2018, 15, 5349−5360

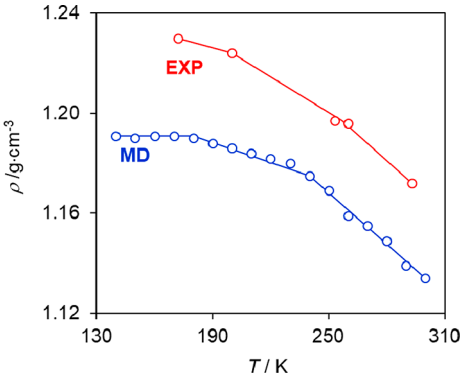

Figure 9. Densities of simvastatin, obtained from the single crystal X-ray diffraction data determined in this work (EXP, Table 1) and from molecular dynamics (MD) simulations. The lines are just to guide the eye.

between both sets of results is excellent, namely, the phase transitions separating the stability domains of the three polymorphs are clearly evidenced by changes in slope of the ρ-T curves. In the case of the MD results, the III → II and II → I transitions are observed at approximately 180 and 240 K, respectively. Albeit these temperatures are lower by 56 and 35 K, respectively, from T_{on}(III → II) = 235.9 ± 0.1 K and T_{on}(II → I) = 275.2 ± 0.2 K obtained by DSC (Figure 3), it is nevertheless remarkable that the simulations were able to capture the existence of the two phase transitions using such a nonspecifically parametrized force field. Indeed, except for the atomic point charges, which were derived from ab initio calculations on simvastatin,[11] all the remaining parameters were directly taken from the OPLS-AA model.[27] In agreement with the above-discussed SCXRD results, the simulations indicated that, apart from intermolecular distance changes directly linked to lattice expansion, the positions of the simvastatin molecules in the unit cell are essentially the same at all temperatures and the differences between the three forms are primarily originated by the increase in the number of accessible conformations of the D1 and D2 dihedral angles as the temperature increases. This last feature was evidenced by the analysis of Figure 10, which shows the combined D1−D2 distribution functions for the *A* and *B* molecules calculated at selected temperatures from the MD results (recall that all calculations were started from a simulation box corresponding to the twinned single crystal structure determined at 172 K, where half of the molecules are with the ester tail in conformation *A* and another half in conformation *B*, see Table 2). In the 140−200 K range covering the III → II phase transition: (i) At 140 K (before the transition), the ester tails of the *A* and *B* molecules preferentially adopt D1 conformations close to 180° and 130°, respectively. These values are in good agreement with those experimentally found by SCXRD for form III at 172 ± 2 K and 200 ± 2 K namely, ∼175° for molecule *A* and ∼129° for molecule *B* (Table 2). (ii) At 200 K (after but close to the transition), the D1 dihedral angle is essentially found close to ±20° and 180° in molecule *A* and in the range 110−180° for molecule *B*. These preferences also encompass those experimentally found for the form II structures obtained at 253 ± 2 K (130.5°, 175.4°; resolved disorder) and 260 ± 2 K (130.5°, 143.3°; unresolved disorder), where the distinction between molecules *A* and *B* could no longer be noticed (this aspect is further discussed below).

For the D2 dihedral angle, in the same temperature domain (140−200 K), no clear correlation between the experimental and theoretical results is noticed. This is, however, not unexpected, given, on the one hand, the empirical nature of the force field used in the simulations and, on the other hand, the uncertainty in the SCXRD determination of those dihedral angles, reflected by large thermal ellipsoids of the atoms in the simvastatin ester tail (Figure 6). Nevertheless, the overall picture conveyed by Figure 10 clearly suggests that at the molecular level the III → II transition is essentially related with an increase in the range of accessible D1 and D2 dihedral angles as the tempeature increases.

One additional interesting aspect in the context of the III → II transition, reflected by Figure 10, is that two molecules with different dihedral preferences can still be distinguished on entering the form II domain and that this distinction is

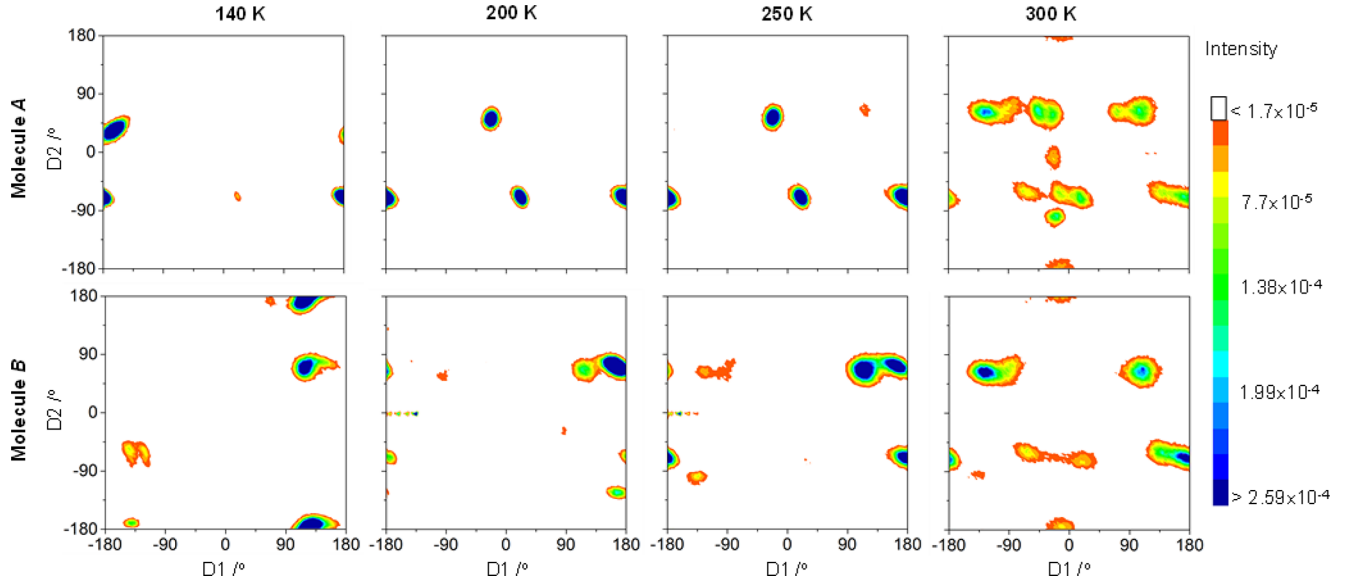

Figure 10. Combined distribution functions for the D1 and D2 dihedral angles of the simvastatin ester tail (see Figure 1), computed from the molecular dynamics simulation results. The illustration shows the evolution of the D1 and D2 distributions when a crystal initially corresponding to the twinned structure determined in this work at 172 K (two molecules, *A* and *B*, in the asymmetric unit) is heated from 140 to 300 K.

DOI: 10.1021/acs.molpharmaceut.8b00818
Mol. Pharmaceutics 2018, 15, 5349−5360

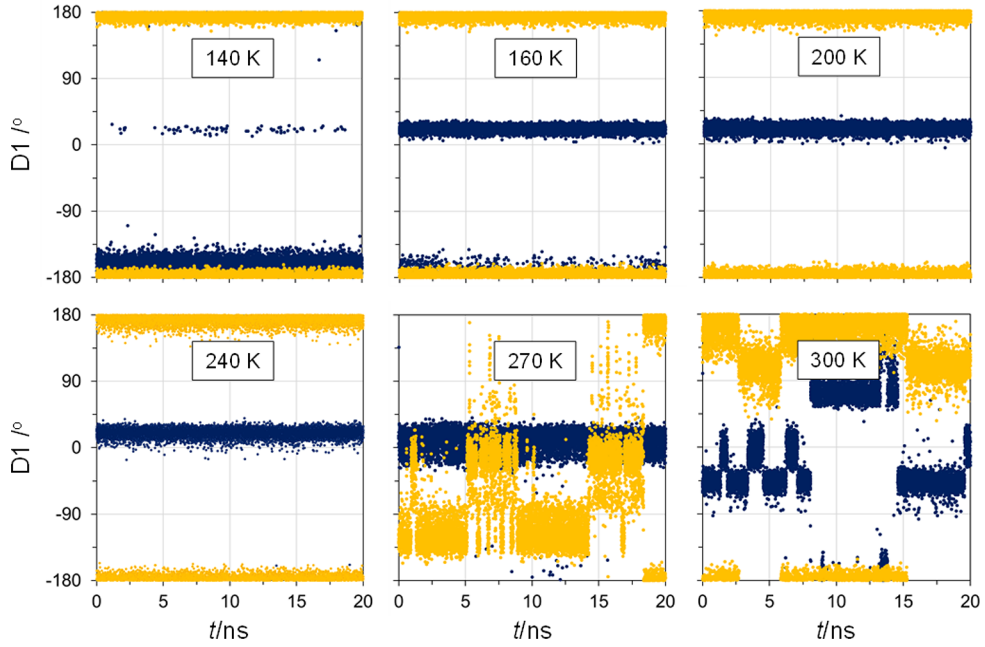

Figure 11. Variation of the dihedral angle D1 along the 20 ns production stage of the MD simulations, for two simvastatin molecules (yellow dots and blue dots), and for different temperatures. The simulations were started at 140 K with the two molecules in the conformation of the *A* molecule in the asymmetric unit of the experimental form III twinned structure at 172 K.

progressively blurred as the temperature increases. This is in good agreement with previously reported ^{13}C CP/MAS NMR results showing that doublet peaks corresponding to two distinct conformation states of the ester tail are still observed above the III → II transition, and that they progressively merge into a single peak as the temperature raises within the form II domain.[14] It is also consistent with the fact that the attempts carried out in this work to obtain the molecular and crystal structure of simvastatin at 240 K (slightly above the temperature of the III → II phase transition) from SCXRD analysis failed. Probably due to the presence of different forms in the same crystal, the acquired data was always of very poor quality, R(int) = 0.4405. Structure determinations as a twin crystal, in $P2_1$ monoclinic space group, or as a $P2_12_12_1$ orthorhombic form were equally dissatisfactory. In both cases the carbon atoms of the ester tail in the electron density map could not be located and the final refinements led to R values over 0.20 and to nonpositive definite atoms positions. It can therefore be concluded that all evidence from the MD simulations, SCXRD, and heat capacity measurements carried out in this work, and from the reported ^{13}C CP/MAS NMR experiments, support the view that the form II domain is characterized by a continuous increase in the variability of conformations accessible to the simvastatin ester tail as the temperature increases, without any large enough discontinuity to originate a detectable phase transition. Note that the SCXRD structures of form II here reported at 253 ± 2 K and 260 ± 2 K, and the published one obtained by PXRD-SR at 258 K,[14] correspond to temperatures above 247 K, where the ^{13}C CP/MAS NMR results show no evidence of peak splitting signaling the possible existence of two molecules with different dihedral preferences.[14]

Figure 10 also indicates that the II → I phase transition is accompanied by a complete change in D1 and D2 patterns. Indeed, the plots at 250 and 300 K show that molecules starting the simulation at 140 K, with either an *A* or a *B* conformation, cannot be distinguished in terms of D1 and D2 preference. This observation is in line with our previous MD results for temperatures above ambient, where a high mobility of the simvastatin ester tail could clearly be noticed.[11]

To obtain further insights into the molecular dynamics of the phase transitions, the D1 and D2 dihedral angles for each molecule in the simulation box were computed for all frames collected during the 20 ns production time, at each temperature. A similar behavior was found for the two angles, independently of the initial position of the molecules in the asymmetric unit (*A* or *B*). The corresponding D1 versus time plots are illustrated in Figure 11. Because of the large volume of data, only the results for two molecules (yellow and blue) with an initial *A* conformation, at six representative temperatures, are shown. The corresponding distributions for all *A* molecules in the simulation box are given as Supporting Information. At 140 K most of the molecules have the D1 and D2 dihedral angles oscillating around their initial equilibrium positions. Nevertheless, as illustrated by the blue dots some of them can, for brief moments, undergo large D1 amplitude changes (ΔD1≈180°) and then return to the initial position. This is also valid for D2 and occurs for ∼40% of the molecules (Figure S2 of the Supporting Information). As the temperature increases the blue dots show a progressive shift toward a new D1 preference (Figure 11, 160 K), which is finally adopted upon completion of the III → II phase transition (Figure 11, 200 K). The number of accessible D1 (and D2) conformations for the molecule corresponding to the blue dots continues to increase with temperature along the form II domain until close to the II → I phase transition temperature (Figure 11, 240 K). Interestingly, no such changes are noted for the molecule represented by the yellow dots, which approximately maintains the same configurational preference until the onset of the II → I transition. When the stability domain of form I is reached, all molecules in the simulation box start to display significant D1 (and D2) changes, which increase as the temperature increases (Figure 11, 240 K). The ester tails remain at a specific position for a few

DOI: 10.1021/acs.molpharmaceut.8b00818
Mol. Pharmaceutics 2018, 15, 5349−5360

nanoseconds and then switch to a new conformation (Figure 11, 270 and 300 K).

In summary, consistent with the experimental evidence discussed in previous sections, the MD simulation results also suggest that the three simvastatin forms are very similar from a packing point of view and that their main differences rely on changes in the conformational dynamics of the ester tail in different temperature ranges.

CONCLUSIONS

The present work confirmed the existence of three simvastatin polymorphs: form III corresponding to a pseudomerohedral twinned monoclinic structure ($P2_1$, $Z'/Z = 2/4$, twin fraction $x = 0.5$), stable below 235.9 ± 0.1 K; form II, orthorhombic ($P2_12_12_1$, $Z'/Z = 1/4$), stable between 235.9 ± 0.1 K and 275.2 ± 0.2 K; and form I stable from 275.2 ± 0.2 K to the fusion point (412.2 ± 0.2 K). The results also suggest that (i) the three simvastatin polymorphs exhibit a very similar molecular packing and their main structural differences seem to result from the dynamics of the "ester tail" movement, which is essentially frozen in two conformations below the III → II transition temperature, becomes progressively less hindered throughout the stability domain of form II, and acquires considerable rotation freedom above the II → I transition; (ii) the III ↔ II and II ↔ I transitions are both fast, reversible, and enantiotropic; (iii) they occur under single crystal to single crystal conditions, without any signs of crystal fragmentation, and with small variations in unit cell volume (<2% if thermal expansion to a common temperature is considered); (iv) the migration of an interface could be clearly noted by hot stage microscopy at the phase transition onsets, thus suggesting a nucleation and growth mechanism. (v) Last but not the least from a pharmaceutical point of view, the fact that the two transitions are fast and reversible with very small hysteresis between cooling and heating modes indicates that the existence of different crystalline forms should not significantly affect the production of simvastatin solid dosage forms. Indeed, the III and II forms are metastable at ambient temperature and, if present, will readily convert to form I, whose stability domain extends up to the fusion temperature. It should, nevertheless, be bear in mind that melting and quench cooling can lead to persistent amorphous phases,[35,36] or to chemical degradation,[37] if the process is not carried out under inert atmosphere. The possibility of chemical degradation will be particularly critical if, for example, strategies to improve the solubility of simvastatin involving melting are considered.

ASSOCIATED CONTENT

Supporting Information

The Supporting Information is available free of charge on the ACS Publications website at DOI: 10.1021/acs.molpharmaceut.8b00818.

Detailed DSC results; results of accuracy test to heat capacity measurements with benzoic acid and of heat capacity measurements on simvastatin; MD simulation results (PDF)

CIF file with single crystal X-ray diffraction structures of simvastatin obtained at different temperatures (CIF)

Video images of the phase transitions recorded in the HSM experiments (AVI)

Video images of the phase transitions recorded in the HSM experiments (AVI)

Video images of the phase transitions recorded in the HSM experiments (AVI)

AUTHOR INFORMATION

Corresponding Author

*E-mail: memp@fc.ul.pt. Phone. +351-21-7500866. Fax +351-21-7500088.

ORCID

Ricardo G. Simões: 0000-0003-4989-4087

Carlos E. S. Bernardes: 0000-0003-1490-9728

Franziska Emmerling: 0000-0001-8528-0301

Manuel E. Minas da Piedade: 0000-0001-7550-6952

Notes

The authors declare no competing financial interest.

ACKNOWLEDGMENTS

This work was supported by Fundação para a Ciência e a Tecnologia (FCT), Portugal thorough projects LISBOA-01-0145-FEDER-028401 and PEst-OE/QUI/UI0100/2013, and grants awarded to A.J. (SFRH/BD/90386/2012), R.G.S. (SFRH/BPD/118771/2016), and C.E.S.B. (SFRH/BPD/101505/2014). We also acknowledge COST Action CM1402.

REFERENCES

(1) Li, J. J. *Triumph of the heart. The story of statins*; Oxford University Press: New York, 2009; pp 28−30.

(2) The Top 200 Drugs of 2018. *ClinCalc DrugStats Database 2018*; ClinCalc LLC, 2018. http://clincalc.com/DrugStats/Top200Drugs.aspx (accessed September 2018).

(3) Granik, V. G. Some chemical and biochemical aspects of the problem of atherosclerosis. *Pharm. Chem. J.* **2012**, *46*, 139−153.

(4) Vance, D. E. Cholesterol in the year 2000. *Biochim. Biophys. Acta, Mol. Cell Biol. Lipids* **2000**, *1529*, 1−8.

(5) Roger, V. L.; Go, A. S.; Lloyd-Jones, D. M.; Benjamin, E. J.; Berry, J. D.; Borden, W. B.; Bravata, D. M.; Dai, S.; Ford, E. S.; Fox, C. S.; Fullerton, H. J.; Gillespie, C.; Hailpern, S. M.; Heit, J. A.; Howard, V. J.; Kissela, B. M.; Kittner, S. J.; Lackland, D. T.; Lichtman, J. H.; Lisabeth, L. D.; Makuc, D. M.; Marcus, G. M.; Marelli, A.; Matchar, D. B.; Moy, C. S.; Mozaffarian, D.; Mussolino, M. E.; Nichol, G.; Paynter, N. P.; Soliman, E. Z.; Sorlie, P. D.; Sotoodehnia, N.; Turan, T. N.; Virani, S. S.; Wong, N. D.; Woo, D.; Turner, M. B.; Comm, A. H. A. S.; Subcomm, S. S. Heart disease and stroke statistics-2012 update A report from the American heart association. *Circulation* **2012**, *125*, E2−E220.

(6) Taylor, F.; Ward, K.; Moore, T. H. M.; Burke, M.; Davey Smith, G.; Casas, J. P.; Ebrahim, S. *Statins for the Primary Prevention of Cardiovascular Disease*; Cochrane Database of Systematic Reviews 2011; John Wiley: New York, 2012; (1) CD004816.

(7) Bernstein, J. *Polymorphism in Molecular Crystals*; Oxford University Press: Oxford, 2002.

(8) Hilfiker, R. *Polymorphism in the Pharmaceutical Industry*; Wiley-VCH Verlag GmbH & Co.: Weinheim, 2006.

(9) Brittain, H. G. *Polymorphism in Pharmaceutical Solids*; Marcel Dekker: New York, 1999.

(10) Brittain, H. G. *Polymorphism in Pharmaceutical Solids*, 2nd ed.; Informa Healthcare USA, Inc.: New York, 2009.

(11) Simões, R. G.; Bernardes, C. E. S.; Diogo, H. P.; Minas da Piedade, M. E. Energetics of simvastatin. *Mol. Pharmaceutics* **2013**, *10*, 2713−2722.

(12) Groom, C. R.; Bruno, I. J.; Lightfoot, M. P.; Ward, S. C. The Cambridge Structural Database. *Acta Crystallogr., Sect. B: Struct. Sci., Cryst. Eng. Mater.* **2016**, *B72*, 171−179.

DOI: 10.1021/acs.molpharmaceut.8b00818
Mol. Pharmaceutics 2018, 15, 5349−5360

(13) Čejka, J.; Kratochvíl, B.; Císařová, I.; Jegorov, A. Simvastatin. *Acta Crystallogr., Sect. C: Cryst. Struct. Commun.* **2003**, *C59*, O428−O430.
(14) Hušák, M.; Kratochvíl, B.; Jegorov, A.; Brus, J.; Maixner, J.; Rohlíček, J. Simvastatin: structure solution of two new low-temperature phases from synchrotron powder diffraction and ss-NMR. *Struct. Chem.* **2010**, *21*, 511−518.
(15) Tan, N. Y.; Zeitler, J. A. Probing phase transitions in simvastatin with terahertz time-domain spectroscopy. *Mol. Pharmaceutics* **2015**, *12*, 810−815.
(16) *SADABS; Area-Detector Absorption Correction*; Bruker AXS Inc.: Madison, 2004.
(17) *SAINT: Area-Detector Integration Software (version 7.23)*; Bruker AXS Inc.: Madison, 2004.
(18) Sheldrick, G. M. Crystal structure refinement with SHELXL. *Acta Crystallogr B* **2015**, *C71*, 3−8.
(19) Sheldrick, G. M. *SHELXL-97: Program for the Refinement of Crystal Structure*; University of Göttingen: Germany, 1997.
(20) Farrugia, L. J. WinGX suite for small-molecule single-crystal crystallography. *J. Appl. Crystallogr.* **1999**, *32*, 837−838.
(21) Macrae, C. F.; Bruno, I. J.; Chisholm, J. A.; Edgington, P. R.; McCabe, P.; Pidcock, E.; Rodriguez-Monge, L.; Taylor, R.; van de Streek, J.; Wood, P. A. Mercury CSD 2.0 - new features for the visualization and investigation of crystal structures. *J. Appl. Crystallogr.* **2008**, *41*, 466−470.
(22) Spek, A. L. *PLATON, A Multipurpose Crystallographic Tool*; Utrecht University: Utrecht, The Netherlands, 2007.
(23) Martinho Simões, J. A.; Minas da Piedade, M. E. *Molecular Energetics: Condensed Phase Thermochemical Techniques*; Oxford University Press: New York, 2008; pp 182−183.
(24) Joseph, A.; Bernardes, C. E. S.; Minas da Piedade, M. E. Heat capacity and thermodynamics of solid and liquid pyridine-3-carboxylic acid (nicotinic acid) over the temperature range 296 to 531 K. *J. Chem. Thermodyn.* **2012**, *55*, 23−28.
(25) Furukawa, G. T.; McCoskey, R. E.; King, G. J. Calorimetric properties of benzoic acid from 0-degrees-K to 410-degrees-K. *J. Res. Natl. Bur. Stand.* **1951**, *47*, 256−261.
(26) Abraham, M. J.; Murtola, T.; Schulz, R.; Páll, S.; Smith, J. C.; Hess, B.; Lindahl, E. GROMACS: High performance molecular simulations through multi-level parallelism from laptops to supercomputers. *SoftwareX* **2015**, *1−2*, 19−25.
(27) Jorgensen, W. L.; Maxwell, D. S.; Tirado-Rives, J. Development and testing of the OPLS all-atom force field on conformational energetics and properties of organic liquids. *J. Am. Chem. Soc.* **1996**, *118*, 11225−11236.
(28) Kaminski, G.; Jorgensen, W. L. Performance of the AMBER94, MMFF94, and OPLS-AA force fields for modeling organic liquids. *J. Phys. Chem.* **1996**, *100*, 18010−18013.
(29) Bernardes, C. E. S.; Joseph, A. Evaluation of the OPLS-AA force field for the study of structural and energetic aspects of molecular organic crystals. *J. Phys. Chem. A* **2015**, *119*, 3023−3034.
(30) Bernardes, C. E. S. AGGREGATES: Finding structures in simulation results of solutions. *J. Comput. Chem.* **2017**, *38*, 753−765.
(31) Meija, J.; Coplen, T. B.; Berglund, M.; Brand, W. A.; De Bievre, P.; Groning, M.; Holden, N. E.; Irrgeher, J.; Loss, R. D.; Walczyk, T.; Prohaska, T. Atomic weights of the elements 2013 (IUPAC Technical Report). *Pure Appl. Chem.* **2016**, *88*, 265−291.
(32) Brus, J. Personal communication.
(33) Sahoo, S. C.; Sinha, S. B.; Kiran, M. S. R. N.; Ramamurty, U.; Dericioglu, A. F.; Reddy, C. M.; Naumov, P. Kinematic and mechanical profile of the self-actuation of thermosalient crystal twins of 1,2,4,5-tetrabromobenzene: A molecular crystalline analogue of a bimetallic strip. *J. Am. Chem. Soc.* **2013**, *135*, 13843−13850.
(34) Bernardes, C. E. S.; Minas da Piedade, M. E.; Canongia Lopes, J. N. Polymorphism in 4′-hydroxyacetophenone: A molecular dynamics simulation study. *J. Phys. Chem. B* **2012**, *116*, 5179−5184.
(35) Graeser, K. A.; Strachan, C. J.; Patterson, J. E.; Gordon, K. C.; Rades, T. Physicochemical properties and stability of two differently prepared amorphous forms of simvastatin. *Cryst. Growth Des.* **2008**, *8*, 128−135.
(36) Nunes, T. G.; Viciosa, M. T.; Correia, N. T.; Danede, F.; Nunes, R. G.; Diogo, H. P. A stable amorphous statin: Solid-state NMR and dielectric studies on dynamic heterogeneity of simvastatin. *Mol. Pharmaceutics* **2014**, *11*, 727−737.
(37) Simões, R. G.; Diogo, H. P.; Dias, A.; Oliveira, M. C.; Cordeiro, C.; Bernardes, C. E. S.; Minas da Piedade, M. E. Thermal stability of simvastatin under different atmospheres. *J. Pharm. Sci.* **2014**, *103*, 241−248.

DOI: 10.1021/acs.molpharmaceut.8b00818
Mol. Pharmaceutics 2018, 15, 5349−5360